Technical Note N-1334

SHORT-TERM ENGINEERING BEHAVIOR OF A DEEP-SEA CALCAREOUS SEDIMENT

by

P. J. Valent

March 1974

Sponsored by
OFFICE OF NAVAL RESEARCH

CIVIL ENGINEERING LABORATORY
Naval Construction Battalion Center
Port Hueneme, California 93043

UNCLASSIFIED

SECURITY CLASSIFICATION OF THIS PAGE (When Data Entered)

REPORT DOCUMENTATION PAGE		READ INSTRUCTIONS BEFORE COMPLETING FORM
1. REPORT NUMBER TN-1334	2. GOVT ACCESSION NO.	3. RECIPIENT'S CATALOG NUMBER
4. TITLE (and Subtitle) Short-Term Engineering Behavior of a Deep-Sea Calcareous Sediment		5. TYPE OF REPORT & PERIOD COVERED Not final
		6. PERFORMING ORG. REPORT NUMBER
7. AUTHOR(s) P. J. Valent		8. CONTRACT OR GRANT NUMBER(s)
9. PERFORMING ORGANIZATION NAME AND ADDRESS CIVIL ENGINEERING LABORATORY Naval Construction Battalion Center Port Hueneme, California 93043		10. PROGRAM ELEMENT, PROJECT, TASK AREA & WORK UNIT NUMBERS 42-009
11. CONTROLLING OFFICE NAME AND ADDRESS Office of Naval Research Arlington, VA 22217		12. REPORT DATE March 1974
		13. NUMBER OF PAGES 36
14. MONITORING AGENCY NAME & ADDRESS(if different from Controlling Office)		15. SECURITY CLASS. (of this report) Unclassified
		15a. DECLASSIFICATION/DOWNGRADING SCHEDULE

16. DISTRIBUTION STATEMENT (of this Report)

Approved for public release; distribution unlimited.

17. DISTRIBUTION STATEMENT (of the abstract entered in Block 20, if different from Report)

18. SUPPLEMENTARY NOTES

19. KEY WORDS (Continue on reverse side if necessary and identify by block number)

Sediments
Oozes
Calcareous ooze
Ocean bottom
Soil mechanics
Soil properties

20. ABSTRACT (Continue on reverse side if necessary and identify by block number)

The engineering index parameters, primary consolidation properties, and effective-stress strength properties of a deep-sea calcareous sediment are reported. This short-term engineering property description of the sediment is the first stage of an in-depth study of creep behavior of this sediment during consolidation and shear. The calcareous sediment sample has been classified as an inorganic silt, according to the Unified Soil Classification System. The compression index, C_c, is 0.80; empirical correlations from

DD FORM 1 JAN 73 1473 EDITION OF 1 NOV 65 IS OBSOLETE

UNCLASSIFIED

SECURITY CLASSIFICATION OF THIS PAGE (When Data Entered)

20. Continued.

terrestrial engineering between C_c and other, easily and rapidly-measured index parameters may be in error by 30%. The effective angle of internal friction, $\bar{\phi}$, of the sediment, when normally consolidated, is 0.65 radians (37 degrees). No significant crushing of the hollow Foraminifera tests (shells) comprising the coarse-size fraction of the sediment was noted in the consolidation tests up to stresses of 1530 kPa (32,000 psf). It was demonstrated, however, that this coarse-size fraction does undergo significant crushing if the material finer than 0.043 millimeter is removed, suggesting that the fine-size fraction acts to distribute load on the coarse-size, test (shell) surfaces.

INTRODUCTION

This interim report describes procedures used and findings to date regarding the engineering behavior of a deep-sea calcareous ooze, composed primarily of Globigerina foraminifera tests.

The report describes the results of physical property, engineering index parameter, one-dimensional consolidation, and triaxial shear strength (undrained) testing. Examination of the drained shear strength behavior, shear creep and secondary consolidation performance, and the accompanying changes in sediment grain character is underway; the results will be summarized in a subsequent report.

BACKGROUND

Sediment Description

Calcareous oozes are seafloor sediments containing more than 30% calcium carbonate [1]. Such oozes cover approximately 36% of the seafloor and are generally restricted to water depths less than 4,500 m (14,000 ft) [2]. The calcareous fraction of these sediments, which may be as large as 97% of the whole by weight [3], is composed primarily of the skeletal remains of various plankton animals and plants of which the foraminifera Globigerina predominates.

The most widely distributed sizes of Globigerina tests are 0.05 to 0.25 mm [4], although Globigerina tests of 1 mm diameter are common in the Caribbean samples of the subject study. The coarse-grained sediment fraction of predominantly whole tests is mixed in varying proportion with a finer-grained fraction composed of foraminifera test fragments; other marine life remains, such as those of the Coccolithophoridae and the nannoplankton (dwarf plankton); inorganic-origin material, such as the clay minerals; and minor additional components [1].

Objective

It is the purpose of this study to examine the consolidation and shear creep behavior of a calcareous deep-sea sediment, composed in large part of Globigerina foraminifera; to evaluate that behavior with respect to observed sediment grain character changes; and to propose a generalized behavioral model for similar deep-sea sediments.

Definitions

Soil response to a change in the applied stress field may be ideally divided into two components: consolidation, involving soil element volume change under hydrostatic stress; and shear deformation, involving soil element shape deformation with no accompanying volume change. (The term ‘‘element’’ refers to an assemblage of soil particles and associated pore fluid.)

Consolidation is, by convention, further divided into three components of volume change: an initial component due to the compression of the gaseous phase in the soil voids, termed immediate compression; an intermediate component governed by the hydrodynamic lag of the soil pore fluid in exiting the soil mass, termed primary consolidation; and a final component governed essentially by a relaxation of interparticle bonds, whatever may be their nature, and slight slippages and dislocations of particles in the soil structure, termed secondary consolidation.

Idealized soil shear deformation or volume deformation without volume change, is generally characterized by a non-linear stress-strain response during which time the soil particles are rearranging themselves in response to the applied stress field. Failure in shear is identified by the occurrence of a peak shearing stress condition or by the occurrence of excessive shearing deformations. However, even when the application of the shearing load to the soil element is halted prior to failure, relaxation of interparticle bonds and reorientation of particles will continue, manifested as soil element deformations at decreasing, constant, or increasing rates. This time-dependent soil shape deformation, without volume change, under constant shearing load is termed shear creep.

Previous Examination

Most seafloor sediment examination has been confined to the measurement of bulk wet density, grain size distribution, specific gravity of the grains, Atterberg limits, carbonate content, organic carbon content, color, odor, and a strength index [5-8]. Several investigations have been performed to define the consolidation characteristics of calcareous oozes, but these have not evaluated the secondary consolidation characteristics [9-12], and further, the sediment involved in some of these is believed to be [9, 11, 12] a precipitate, not an organic construction. Only one in-depth study of consolidation, including secondary consolidation, of a ‘‘deep-sea sediment’’ is known [13]; that sediment was probably terrigeneous in origin and contained little calcareous material. No study of shear creep deformation behavior of a deep-ocean sediment has been published.

Approach

Samples of a calcareous ooze have been obtained and are being evaluated via conventional soils testing and data analysis techniques. Physical property and engineering index parameter tests have been completed and the data evaluated in order to compare the pelagic sediment samples with terrestrial soils. Test results describing the primary consolidation behavior have been evaluated and are presented herein, followed by the results of short-term shear deformation tests describing the shear failure condition of the sediment.

The secondary consolidation and shear creep behavior of this material are the subject of present testing and evaluation, to be published at a later date. The secondary consolidation behavior of many soils has been examined by others with the intention of developing a satisfactory universal treatment of the phenomenon [14-21], but none of these treatments has proven universally successful (Reference 22, p. 142). Similarly, the shear creep phenomenon has been examined by others in many soils [23-27], but the fundamental concepts needed to develop practical design tools to control creep effects are not yet available (Reference 22, p. 144). This future study will examine the applicability to calcareous ooze of the previously developed predictive techniques for secondary consolidation and shear creep phenomena, and will evaluate sediment grain character changes during consolidation and shear creep to assist in understanding and developing a predictive model for calcareous ooze load-deformation-time behavior.

SAMPLE ACQUISITION AND INDEX PROPERTIES

Coring and Core Transport and Storage

Calcareous ooze samples were obtained from the USNS WILKES in the central Caribbean (Venezuelan Basin) approximately at latitude 15°00'N, longitude 69°20'W. It was desirable for this study to obtain samples of large horizontal area to provide adjacent test specimens from the same horizontal strata, that is, to provide specimens of near identical initial condition. Thus, a spade box corer [28], (see Figure 1) with a sample box 0.20 x 0.30 x 0.46 m high, was used to obtain two cores at each of two sites (four cores total) about 7.5 km (4 naut. mi.) apart in 3,930 m water depth. Topography slopes gently upward to the northwest with no significant undulations (i.e., no abyssal hills). The box corer samples included material from sediment depths of 30-490 mm to 100-560 mm depending on the depth of corer penetration; that is, corer tip penetration varied from 490 to 560 mm. The driving head to which the core box is fastened permits clearance for the 100 mm of material above the core box resulting from overpenetration. Thus, the overpenetration does not cause the core sample to be contorted or compacted.

On deck, excess material above the core box top was struck off level (Figures 2 and 3). Then two procedures for sample storage were followed. One of the box cores from each site was capped with a flat plate and then wrapped tightly in three separate sheets of 10-mil polyvinyl chloride (PVC) sealed with tape (Figure 4). Each of these packages, weighing about 59 kg (130 lbs), was immersed in seawater in a 30-gallon trash can. The second box core from each site was cored six times using a piston from a modified Ewing corer and cellulose acetate butyrate (CAB) thinwall tubing (see Figure 5). Tubing size is about 59mm I.D. and 62mm O.D. (2-5/16-in. and 2-7/16-in. respectively). These tubes were trimmed flush with the enclosed sample, capped with snug fitting pipe caps, the caps sealed with electrical tape, the entire tube exterior sealed using a spray paint designed for that purpose, and the ends of the tubes waxed. Water content, Atterberg limit, and grain size samples were taken at three depths in the remaining material. The box cores in seawater, the tube samples, and the index property samples were all stored in the ship scientists' chill locker at $2^{o}C$ ($36^{o}F$).

In order to transport the two plastic-wrapped, box core samples by air as perishable cargo, a cargo weight limit per piece had to be met, requiring the removal of the immersing seawater from the trash cans. This action permitted the pore water of the box cores to drain into the space between the stainless steel box and the enclosing plastic wraps. The resulting change in sample stress state, in turn, caused the sediment to consolidate in the vertical direction as shown by the following data.

The 59-mm-diameter x 460-mm-long tube samples, transported vertically throughout, had lost no water but the solid material had settled 5.7 mm average, apparently due primarily to vibration in transit. The 0.20 x 0.30 x 0.46-m-high box samples on the other hand had no free water on their tops (for that water can drain out of the box between the side walls and the bottom cover) and had settled 10.6 mm and 15.5 mm (Figure 6). Further, faint ''ripple markings'' were noted in the core top surface suggesting that some of the sediment settlement occurred in the ship's chill locker before the immersing seawater was removed.

For the purposes of this study, the calcareous ooze samples, as received in the shore laboratory, have proved satisfactory because they have fulfilled the primary sampling requirement of providing a large number of test specimens of near-identical nature. The vibration densification and consolidation which occurred during transport, while undesirable, have not compromised this study of material behavior. The above volume change results have been detailed for the benefit of other persons whose object it may be to measure in-situ properties on core samples; such measurements on calcareous ooze samples from near the sediment surface must be made on-board ship immediately after obtaining the sample.

Bulk Density

In the laboratory, the measured total bulk densities of the two box corer samples were 1,470 and 1,471 kg/m^3 (91.7 and 91.8 pcf). Using these final bulk densities and using the sample settlements measured in the core boxes, the initial total bulk densities, at time of trimming on the WILKES, were backfigured to be 1,454 and 1,460 kg/m^3 (90.8 and 91.1 pcf).

Water Content

Water content measurements made before and after transport are presented in Figures 7 and 8. These values represent the mass lost during drying at 105°C divided by the mass remaining [29]. Correction for salt content has not been made [30], Such correction will raise the calculated water content by 5 to 6%. For example, an uncorrected water content of 87.5% is equivalent to a corrected value of 92.5%. Some variation between the two curves of each figure should be expected because the two curves represent data from different box corer samples, probably separated by several hundred meters distance. However, the change in water content, from the initial state immediately after sampling to the end state at the end of transport, is so marked as to overshadow initial inter-sample differences. An overall reduction in water content is indicated with lesser reductions at the very top and bottom of the box cores. The data of Figure 7, suggesting that the very bottom of the box core increased in water content during transport, may not represent a true water content change during transport. A facies change to coarse shell material occurred at this depth, and the small water content samples may not represent the average properly.

Vane Shear Index

Vane shear measurements were run in the laboratory on the top and one side of box corer sample 4 (Figures 9 and 10). The trend of the strength and sensitivity measurements does not correspond ideally to what one would expect from the water content data in that, for the depth interval from 0 to 75 mm, the vane shear strength decreases with a decrease in sample water content. This variation is believed due to variation of material with depth rather than to differential cementation or disturbance.

Grain Size Distribution

Grain size analyses were conducted by first dispersing wet samples in distilled water and a deflocculant, then conducting a standard hydrometer analysis [29]. After the 24-hour reading these same samples were then wet-washed through sieves [29]. Figure 11 is typical of the lack of agreement between hydrometer and sieve analyses found; this lack of agreement is believed due primarily to the misuse of Stokes' equation in the hydrometer analysis data reduction. Stokes' equation assumes solid, spherical grains [29] whereas the silt size material of this calcareous ooze is composed of hollow, near-spherical foraminifera tests. The use of the specific gravity of the mineral components (true specific gravity) to calculate the fall time of a given size particle, whose bulk specific gravity (including the enclosed voids) is considerably less than the true value, must therefore produce erroneous results. Development of a simple correction procedure is being examined outside of this study. The hydrometer samples were exposed as little as possible to the atmosphere, and no difficulty was encountered with floating grains in the hydrometer settling tube, as noted by others [10].

Specific Gravity and Carbonate Content

True specific gravities were measured (as described in Reference 30) on powdered material in an air comparison pycnometer; values ranged from 2.65 to 2.69. The calcium carbonate content calculated from the measured inorganic carbon content (obtained as described in Reference 30), assuming the inorganic carbon is in the form of calcium carbonate, ranges from 56 to 75% with a mean of 63%. The organic carbon content [31] ranged from 0.16 to 0.33% with an average of 0.26%. The specific gravity determinations and carbon determinations were not corrected for the weights of the initial pore water salt content.

Atterberg Limits and Soil Classification

Atterberg limit determinations were conducted as described in Reference 29. The liquid limit, w_L, was found to range between 66 and 70, and the plastic limit, w_P, between 42 and 57.

The Atterberg limit determinations on this calcareous ooze are questionable because the samples appeared to become wetter during each trial as the sample was manipulated, even though every care was taken to minimize crushing of the hollow tests. It is possible that water can be drawn out of the tests, through the sieve-like surface, and replaced by air, thus providing surficial lubrication without grain crushing. The results of Atterberg limit determinations on such calcareous ooze sediments can be expected to vary considerably between test operators.

In addition to such operator error, error arises from two other sources. First, as the specimens are dried from the natural water content (see Figures 7 and 8) down to the Atterberg limits, the salt concentration of the pore fluid obviously increases; this concentration change affects the sediment interparticle forces and may result in a measurable effect on the Atterberg limit determination. Second, the changing salt concentration also influences the water content correction calculation; and the approximate correction of Reference 30, based upon 3.5% salt, no longer applies. The quantitative and practical significance of these errors has not been evaluated.

This calcareous ooze classifies in the Unified Soil Classification [32] system as MH, an inorganic silt.

CONSOLIDATION CHARACTERISTICS

One-dimensional consolidation properties of three calcareous sediment specimens are presented herein. For a brief review of the one-dimensional consolidation test, including the recommended specimen relative dimensions, the boundary conditions, the loading technique, and the methods of data presentation and analysis, the reader is referred to the Appendix.

Equipment and Procedure Description

Consolidation tests were conducted in two consolidometers, each having its own advantages. One test was conducted in an Anteus consolidometer, capable of applying a backpressure of 210 kPa (30 psi) to the specimen pore water for the purpose of driving any gas bubbles in the sample back into solution. The Anteus unit has a load range capability from 0.38 to 790 kPa (8 psf to 16,500 psf), with the upper limit dictated by the compressed-air line pressure. The Anteus unit also permits the option of using only top drainage and measuring induced excess pore pressures at the bottom of the specimen, thus the point of 100% excess pore pressure dissipation (end of primary consolidation) can be readily identified (see Appendix, Figure 18). The specimen was 57.2 mm diameter by 18.63 mm high (2.25 in. by 0.733 in.), just slightly smaller in diameter than the tube samples. Consolidation specimens are trimmed to diameter by pushing them into a special consolidometer ring with an integral knife edge.

Two other tests were conducted in a Karol-Warner consolidometer, which does not have a backpressure capability. Its load range capability extends from 0.48 to 2,490 kPa (10 psf to 52,000 psf), with the lower limit dictated by the dial indicator plunger force and the upper limit dictated by the compressed-air line pressure. Specimens were 56.9 mm diameter by 19.05 mm high (2.24 in. by 0.75 in.), prepared similarly to that of the Anteus unit.

Consolidation tests were run on material from the fourth box core retrieved (tube cored in the laboratory). The first test was conducted in the Anteus unit, under backpressure, at a room temperature of about 25°C (77°F). At the completion of the 30-day test duration, the original tan sample color had changed to black at the two faces in contact with the filter paper, and the filter paper itself was somewhat decomposed. The sample gave off some hydrogen sulfide odor. The undesirable end condition of this consolidation specimen is believed due to the flourishing of anaerobic, sulfide-producing bacteria at room temperatures, with the organic filter paper providing the major food source. The specimen in the Anteus is sealed from the atmosphere to permit backpressuring; thus the dissolved oxygen in the water cannot be replenished, and the specimen becomes anaerobic.

The second test was conducted in the Karol-Warner unit, without backpressure, with the consolidometer in a walk-in refrigerator whose temperature varied between 3.3 and 10°C (38 and 50°F respectively). (The refrigerator controls have been repaired reducing the temperature range to 1°C (2°F) for future testing.) This test differed from the first in that the Karol-Warner specimen is not sealed, and anaerobic bacterial growth was therefore somewhat retarded at the specimen. Further growth retardation occurred due to the reduced ambient temperature, from 25°C to 10°C. The load-increment ratio for both tests was 1.0 (see Appendix for definition), and the time duration of each increment was also maintained about the same, 24 hours.

Natural Soil Test Results

Volume Change Versus Pressure. The void ratio versus logarithm of vertical effective stress curve, e-log $\bar{\sigma}_v$, for the tests on natural sediments is presented in Figure 12. Void ratio is defined as the volume of voids divided by the volume of solids. For the data presented herein, the volume of voids was calculated from the measured weight of water driven off, assuming 100% saturation; and the volume of solids was calculated from the measured weight of dried solids, including the weight of dried salt. Thus the void ratios herein are too low by 3 to 4% because the salt component is included in the solids phase rather than in the liquid phase. A correction technique for the seawater effect on the calculated void ratios can be found in Reference 30.

The e-log $\bar{\sigma}_v$ curves for the two natural sediment test specimens appear much the same, suggesting (1) that the growth of anaerobic bacteria in the Anteus test specimen, (2) that backpressuring of this particular soil, and (3) that maintained differences in test temperature probably do not have a significant influence on consolidation of the calcareous ooze tested. Alternately, anaerobic growth, backpressuring, and temperature may have compensating effects on the e-log $\bar{\sigma}_v$ function resulting in no net difference in consolidation response. (It is possible that the 210 kPa (30 psi) backpressure was not sufficient to dissolve all bubbles, but it is believed that more obvious behavioral differences than noted would occur if bubbles were a problem.)

The second important observation, from the e-log $\overline{\sigma}_v$ data, is that the curve does not become a straight line at higher pressures as is usually the case (Reference 33, p. 217). Other researchers have found similar behavior in calcareous material [11, 12], while a third paper indicates no continuing curvature [10]. It has been suggested [34] that the effect could be due to the extrusion of material past the porous stone at higher pressures; this possibility is being examined. Volume change versus pressure data are by convention quantified in terms of the slopes of straight line approximations to the e-log $\overline{\sigma}_v$ curve. The slope of the straight line approximation to the latter part of the curve during loading is called the compression index, C_c; and the slope of the curve during unloading is called the swelling index C_s . (See Figure 12.)

The compression index for the two tests on natural calcareous ooze was about 0.80 and the swelling indices were 0.036 and 0.056.

Predictive Capability. Various relationships have been used to estimate the compression index, C_c, for clays. Terzaghi and Peck suggest the relationship

$$C_c = 0.009\ (w_L - 10)\ \text{(Reference 35)}$$

which, assuming an average liquid limit, w_L, of 68 for the calcareous ooze, would indicate a C_c of 0.52 (65% of that measured). A relationship suggested by Herrmann, et al.,

$$C_c = 0.011\ (w_L - 12)\ \text{(Reference 36)}$$

yields a calculated C_c of 0.62 (77% of that measured). These calculated values of C_c compared to the measured value of 0.80, suggest that the calcareous ooze tested is more compressible than a typical clay-type soil having the same liquid limit. On the other hand, other recommended empirical relationships for C_c, based on initial void ratio or on water content, were tested for this calcareous ooze with opposite results. Reference 37 (p. 7-3-12) recommends:

$$C_c = 0.54\ (e_o - 0.35)$$

which for a void ratio, $e_o = 2.71$ yields $C_c = 1.27$ and

$$C_c = 0.0054\ (2.6\ w - 35)$$

which for a water content, w = 97.7%, yields $C_c = 1.18$. These calculated values are half again as large as the measured values.

These discrepancies suggest that calcareous oozes are quite different from terrestrial soils, and that standing empirical relationships for the prediction of soils engineering behavior may not apply. Suggestions can be made regarding reasons for such discrepancies. First, the relationships for predicting C_c based on initial void ratio, e_o, and water content, w, yield values which are too high because much of the water filled voids are within the Globigerina tests and do not substantially enter into the soil compressibility at the loadings used. That the tests do not undergo substantial crushing in the natural specimen is substantiated by a grain size determination made at the conclusion of the second consolidation test; no substantive change in the grain size curves, before and after, could be detected, indicating little crushing. The relationships for predicting C_c based on liquid limit, w_L, yield values which are lower than those measured. Conjecture as to why will be deferred until further testing evaluates the magnitude of error due to sample extrusion around the porous stone; i.e., possibly the observed lack of agreement is due to testing error.

Time Rate of Primary Consolidation. The time rate of consolidation due to each increment of load is obtained by, in effect, comparing the specimen height-change-versus-time curve (for example, see Appendix) with a theoretically-derived curve of volume change versus time as a function of the hydrostatic lag. This comparison is achieved through a curve fitting process and is quantitatively described by an empirical coefficient of consolidation, c_v (see Reference 33, pp. 238-242). The test data obtained for vertical effective stresses, $\bar{\sigma}_v$, less than 96 kPa (2000 psf) were not amenable to these curve fitting procedures. Similar behavior for calcareous ooze has been noted elsewhere [10]. The coefficient of consolidation, for $\bar{\sigma}_v$ equal to and greater than 96 kPa, ranged from 0.003 to 0.021 cm^2/sec.

Time Rate of Secondary Consolidation. After the conclusion of primary consolidation, the specimen height change as a function of time is described quantitatively by the coefficient of secondary consolidation, C_α,

$$C_\alpha = \frac{\Delta H}{H \times \Delta \log_{10} t} \qquad \text{(Reference 38, p. 421)}$$

where $\dfrac{\Delta H}{\Delta \log_{10} t}$ = slope of the secondary consolidation portion of the height change versus log time curve (for example, see Appendix),

H = specimen height at the end of primary consolidation.

Measured values of C_α ranged between 0.0015 and 0.009, with values generally increasing with vertical effective stress. When compared to data from Reference 37 (p. 7-3-15), the above C_α data suggest that the calcareous ooze material undergoes a less-than-average magnitude of secondary consolidation, compared to terrestrial fine-grained soils in general. The secondary consolidation behavior of this sediment and the causes for this behavior are the subject of continuing study.

Artificial Soil Test Results

As indicated earlier, difficulty was experienced in identifying grain crushing in the first two consolidation tests on natural samples. Grain size determination results before and after loading to 1,530 kPa (32,000 psf) suggested no significant changes had occurred. Visual examination revealed holes punched in many test walls both before and after consolidation testing, making an assessment as to the effect of consolidation on test integrity very difficult to substantiate. It was hypothesized that the fine-grained fraction of the ooze material was acting as a load distributor, evenly stressing the tests so as to limit crushing. To test this hypothesis, an artificial sample, with all material passing the No. 325 sieve removed, was consolidation tested as above.

Specimen Preparation. The test sample was prepared by first dispersing material from Box Core 4, 0 to 76mm increment (0 to 3 in.), using distilled water and sodium pyrophosphate. This material was then washed on a 325 sieve using distilled water, while avoiding unnecessary abrasion of the material. (The resulting material, with fines removed, had a specific gravity of 2.79. The specific gravity of calcite is 2.93 and that of aragonite is 2.71 [39].) At the conclusion of washing, the retained material was placed in a beaker of seawater. The seawater-saturated material was then, after a period of equilibrating, spooned into the consolidometer ring of the Karol-Warner unit and then struck off even with the top edge.

Grain Crushing. The e-log $\bar{\sigma}_v$ curve resulting has been plotted in Figure 12, labeled "artificial." The start of the very steep curve is believed to mark the start of significant grain crushing; i.e., between 50 and 200 kPa (about 1,000 and 4,000 psf). The artificial specimen was loaded to 2,420 kPa (50,600 psf) with the test results indicating a C_c of 1.868 and a C_s of 0.030. The results of grain size analyses on the 1-D compression specimen after testing and on the excess sample (which is considered representative of the specimen initial state) are presented in Figure 13. The grain size curves confirm that test crushing did occur in the artificial sample under consolidation. Most crushing occurred in the medium sand size fraction, with 30% of the material being reduced to a size passing the 325 sieve. The results of this third consolidation test confirm the role of the fine-grained fraction in this particular calcareous ooze sample in the protection of the foraminifera tests against crushing.

It is significant to compare the behavior of the artificial calcareous ooze sample with that of a typical terrestrial sand (quartz grains). Similar 1-D consolidation tests on quartz sand indicate the initiation of grain crushing at 14,000 to 21,000 kPa (2,000 to 3,000 psi) (Reference 38, pp. 297, 302), versus 50 to 200 kPa for the calcareous test grains.

SHEAR CHARACTERISTICS

Effective-stress shear strength properties were developed from the results of three triaxial shear tests in which the specimens were consolidated isotropically and then sheared undrained ($\overline{\text{CIU}}$ tests). A brief review of the triaxial test, with terminology defined, is given in the Appendix.

Equipment and Procedure Description

Triaxial shear tests were conducted in conventional equipment (similar to that described in Reference 40) on calcareous ooze specimens 36 mm diameter by 90 mm high (1.4 in. by 3.5 in.). The first shear test, on that specimen consolidated to 37.9 kPa (5.49 psi), used a load ram bushing/seal consisting of two stainless steel linear ball bushings and an O-ring seal [41], which prevented leakage of cell fluid and proved adequate in minimizing friction on the loading ram. Subsequent shear tests have made use of a new load ram bushing/seal, incorporating a compressed air seal, developed at the University of California at Berkeley, which has demonstrated lower ram friction and has yielded smoother and more consistent data curves.

Triaxial specimens cut from the tubes of Box Core 4 were of sufficient strength to support themselves during the trimming and cell assembly process. The samples were provided with filter paper side drains (Reference 40, p. 81) and were enclosed in two rubber membranes separated by silicone grease (Reference 40, p. 39). Tap water was used for the cell fluid and salt water for the specimen pore fluid lines, with the salt water system isolated from the mercury pot system by an oil interface. Cell pressures of about 345 kPa (50 psi) were used throughout, and consolidation pressures were applied by lowering the specimen pressure via the self-compensating mercury control differential pressure system (Reference 40, p. 45-52). Axial loads were applied with a loading frame moving at a constant rate of strain and through a proving ring; the strain rate was such that 20 percent axial strain was completed in about 5-1/2 hours.

Results

<u>Principal Stress Difference</u>. Three specimens were taken from Box Core 4, from about the same elevation in the sample, so that all specimens were of about the same composition and had experienced about the same stress history. These specimens were consolidated to different isotropic stress states by application of consolidation pressure, $\bar{\sigma}_c$, of 6.5, 37.9, and 109.8 kPa (0.94, 5.49, and 15.93 psi). The specimens were then sheared undrained by increasing the principal stress difference $(\sigma_1-\sigma_3)$, that is, by applying an axial load via the load ram. The resulting axial strain response of the three specimens to the change in principal stress difference is presented in Figure 14. The first two specimens ($\bar{\sigma}_c$ = 6.5 and 37.9 kPa) behaved similarly with increasing principal stress difference to 13 to 18% axial strain, after which the principal stress difference remained near constant with strain. These specimens bulged uniformly with continued axial strain, and no shear failure plane could be identified. The third specimen ($\bar{\sigma}_c$ = 109.8 kPa), on the other hand, exhibited a definite peak stress difference, with a reduction of some 15% with continued strain. This specimen exhibited a well-defined failure plane. An examination of foraminifera tests near the failure plane is planned to identify test crushing which may have occurred during this latter shear test, and which could contribute to the strength reduction with axial strain.

<u>Failure Envelope</u>. To determine the significance of these stress-strain data, the relationship $(\sigma_1-\sigma_3)/2$ was plotted versus $(\bar{\sigma}_1+\bar{\sigma}_3)/2$ for the duration of each shear test and is presented in Figure 15. Such a data plot for a shear test is known as a stress path; the quantity $(\sigma_1-\sigma_3)/2$ is a function of the shear stress on a plane within the specimen; and the quantity $(\bar{\sigma}_1+\bar{\sigma}_3)/2$ is a function of the normal stress on that plane (Reference 38, pp. 105-115). The stress paths of Figure 15 are indicative of the stress history of the calcareous ooze material (Reference 38, p. 427). The paths indicate that the specimen consolidated to 6.5 kPa was overconsolidated, in terms of behavior, when sheared; the specimen consolidated to 109.8 kPa was normally consolidated; and the specimen consolidated to 37.9 kPa was intermediate in behavior. A soil element is defined as being normally consolidated if it is at equilibrium under the maximum stress it has ever experienced, and as overconsolidated if it is at equilibrium under a stress less than that to which it was once consolidated (Reference 38, p. 74). The overconsolidated behavior of the first specimen, that consolidated to 6.5kPa, need not necessarily be indicative of the sample condition on the seafloor but may be largely the result of sample state change during coring, transit, storage, and specimen set-up. The source of the behavior will be clarified by future testing of those calcareous ooze samples

shipped in tubes, which experienced less change in sample state (compared to those samples shipped in the corer boxes).

A - Parameters. The ratio of the excess pore pressure to the change in principal stress difference, called the A-parameter [42], has been used as a quantitative measure of sample type and sample state change [42]. A-parameters were calculated at the point of maximum principal stress ratio, $\bar{\sigma}_1/\bar{\sigma}_3$ max.; values of 0.21, 0.75, and 0.89 were obtained for the three samples, in order of increasing consolidation pressure. Skempton [42] suggests that such values, for clay soils, will result from a lightly overconsolidated clay (A_f = 0.21) and from a normally consolidated clay (A_f = 0.75 and 0.89).

Strength Parameters. The data of Figure 15 have been used to produce the Mohr-Coulomb failure envelope for the calcareous ooze sample, represented in Figure 16. Here the ordinate represents the shearing stress on a plane and the abscissa represents the normal stress on that plane. Mohr circles at failure are drawn for each sample and enclosed by the assumed failure envelope. In the normally consolidated region, the angle of internal friction, $\bar{\phi}$, (from $\overline{\text{CIU}}$ tests) is 0.65 radians (37 degrees). This magnitude appears slightly high when compared to $\bar{\phi}$ values found for terrestrial clays (Reference 22, p. 443; Reference 38, p. 215) and silts [43] at comparable void ratios, but a $\bar{\phi}$ = 0.65 radians has been found for other seafloor soils [44, 45, 46].

In the overconsolidated portion of the Mohr envelope, the effective cohesion, $\bar{c}$, is 3.4 kPa (0.5 psi) and the angle of internal friction, $\bar{\phi}$, is 0.58 radians (33 degrees) for the assumed straight line fit to the available two data points.

SUMMARY AND CONCLUSIONS

A deep-sea calcareous ooze has been subjected to a series of laboratory tests in order to classify the sediment with respect to certain physical properties and engineering index parameters. The engineering properties of the sediment have been defined through one-dimensional compression tests and triaxial shear tests, and observations have been made of sediment grain character changes. The testing and evaluation program, now at an intermediate stage, has developed the following conclusions:

1. Although the sediment is called a calcareous ooze, and although it is classified as a sandy clay according to the Trilineal Oceanic Soil Classification system [2], it behaves in an engineering sense as an inorganic silt (Unified Soil Classification System).

2. Calcareous ooze samples should be examined and tested on-board ship immediately after acquisition to the fullest extent

possible (including motorized vane shear testing) because the samples will densify in storage on-board and in transit to the shore laboratory, thus altering their state.

3. One-dimensional consolidation tests on sediment specimens indicate a compression index, C_c, of 0.80. An artificial specimen composed primarily of foraminifera tests had a compression index of 1.87; that is, the artificial specimen was considerably more compressible than the natural specimens.

4. The one-dimensional consolidation tests of the calcareous ooze, which has 40% by weight smaller than 0.002 mm, had negligible observable influence on the Globigerina foraminifera tests (shells) comprising most of the coarser grained size fraction. This response is believed due to the action of the finer grained fraction of the sediment in distributing loads on the foraminifera test surfaces.

5. As demonstrated by the artificial specimen performance, one-dimensional consolidation of calcareous oozes having lesser amounts of fines will, if the coarse Globigerina tests are in contact with each other, result in crushing of the tests and in increased compressibilities at load intensities of engineering interest. This behavior is contrary to that experienced with usual terrestrial soils.

6. The artificial specimen, with the fraction passing the 325 sieve removed, resembles the calcareous oozes found near the tops of seamounts and submarine ridges, where strong currents have removed the fine fraction by winnowing. In such high energy environments, embedment anchors and heavily loaded footing foundations imposing compressive stresses of engineering interest (that is, 50 to 200 kPa or 1,000 to 4,000 psf) will cause crushing of Globigerina tests (shells) making up the coarse-grained calcareous ooze. This grain crushing will manifest itself as large displacements of the anchor or footing, which may impair the function of the structure or may lead to its failure.

7. Empirical relationships used in terrestrial soils engineering for the estimation of the compression index are not directly applicable to calcareous sediments.

8. The coefficient of consolidation, c_v, for vertical effective stresses equal to or greater than 96 kPa (2,000 psf), ranged from 0.003 to 0.021 cm^2/sec. For stresses less than 96 kPa, the end of primary consolidation could not be identified, and, therefore, the value of c_v could not be calculated (using a load increment ratio of 1).

9. The normally-consolidated calcareous ooze sediment exhibits an angle of internal friction, $\bar{\phi}$, of 0.65 radians (37 degrees) in undrained triaxial shear tests.

10. The samples tested from Box Core 4 (sample transported in corer box and tube sampled in the laboratory) behave in shear as an overconsolidated soil when subjected to isotropic consolidation stresses, $\bar{\sigma}_c$, less than about 40 kPa (6 psi). This observed overconsolidation

may or may not be representative of original sediment state in the seafloor.

ACKNOWLEDGMENTS

Assistance in this endeavor has been received from many quarters. Foremost of course is the Office of Naval Research, the sponsor of this work. The Naval Oceanographic Office kindly contributed ship time and space. The Scripps Institution of Oceanography permitted the use of their spade-box corer after only one prep session in its use by Dr. Neil Marshall. The officers and men of the USNS WILKES and the NAVOCEANO scientific complement, especially First Mate Joseph Flaherty and Bosun Patrick Browning, executed a faultless coring operation with a piece of hardware totally new to them. Special thanks are due Mr. F. O. Lehnhardt for his assistance in executing the various laboratory hardware set-up and testing, and Mr. H. J. Lee for his constructive criticism of the drafts of this report.

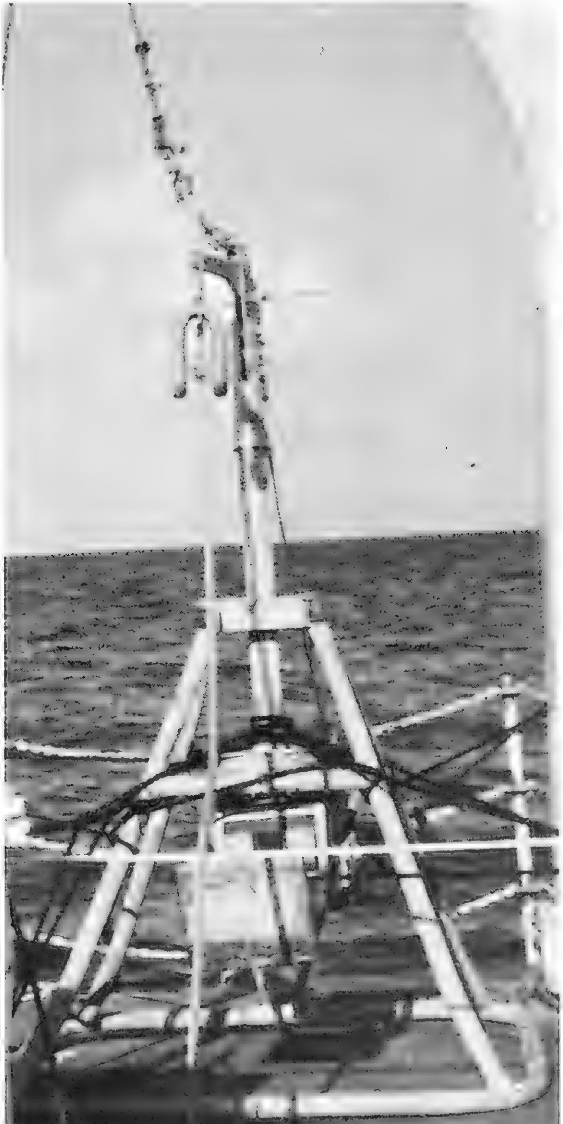

Figure 1. Spade-box corer, corer box not attached.

Figure 2. Full corer box as removed from the corer frame.

Figure 3. Excess surface material being struck off prior to capping and wrapping of the box.

Figure 4. Box core wrapped in three PVC sheets fastened with black and grey tape.

Figure 5. Box core sample after re-sampling with CAB thinwall tubing.

Figure 6. Observed settlement of sample within corer box after partial drainage and disturbance in transit.

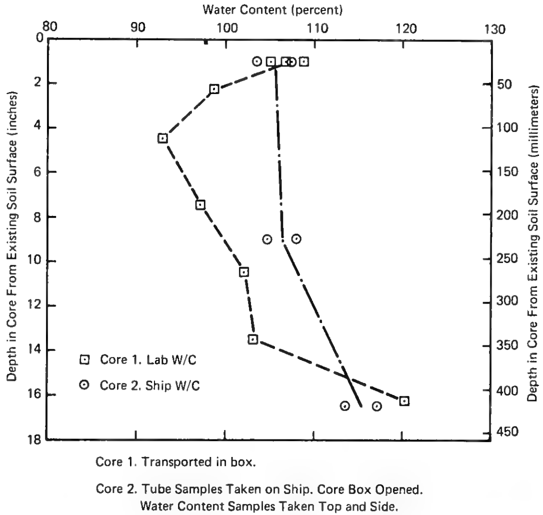

Figure 7. Comparison of box core water content on the ship shortly after coring compared to that in the shore laboratory, Site 1. Comparison indicates sample consolidation and water drainage during storage and transport of box core samples.

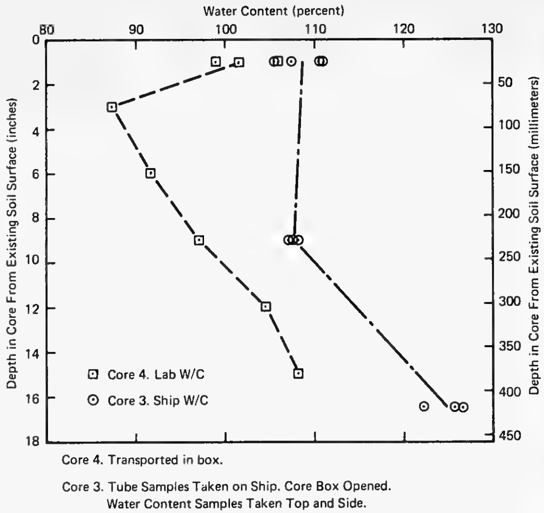

Figure 8. Comparison of box core water content on the ship shortly after coring compared to that in the shore laboratory, Site 2. Comparison indicates sample consolidation and water drainage during storage and transport of box core samples.

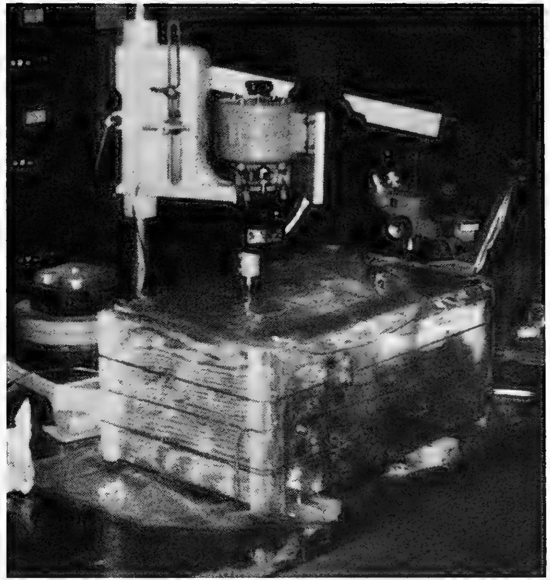

Figure 9. Motorized vane shear test in progress on the side of box core sample, one side of box removed.

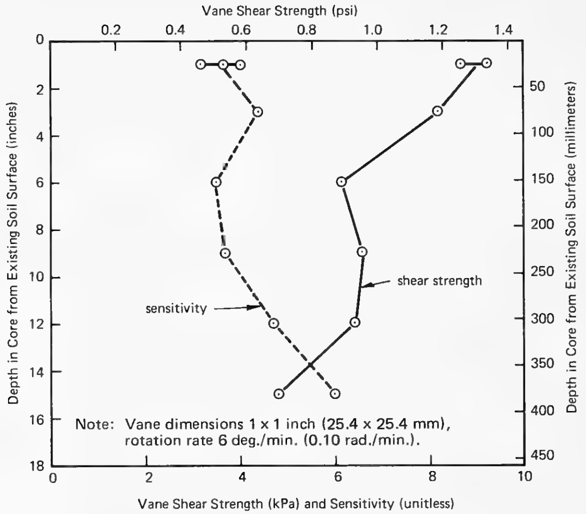

Figure 10. Vane shear strength measurements made on Box Core 4. Measurements at 1-inch (25.4 mm) depth made with core standing vertical, vane entering top; at all other depths core lying on side, vane entering side (see Figure 9).

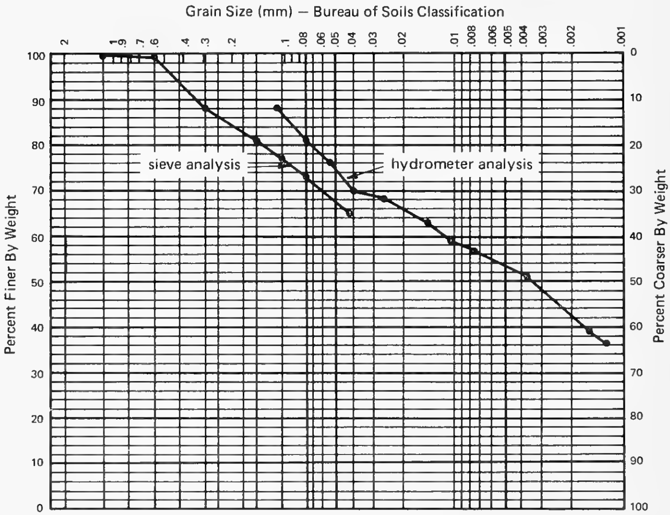

Figure 11. Typical grain size analysis results on specimen from 6 to 9-inch depth (150 to 230 mm) in Box Core 4.

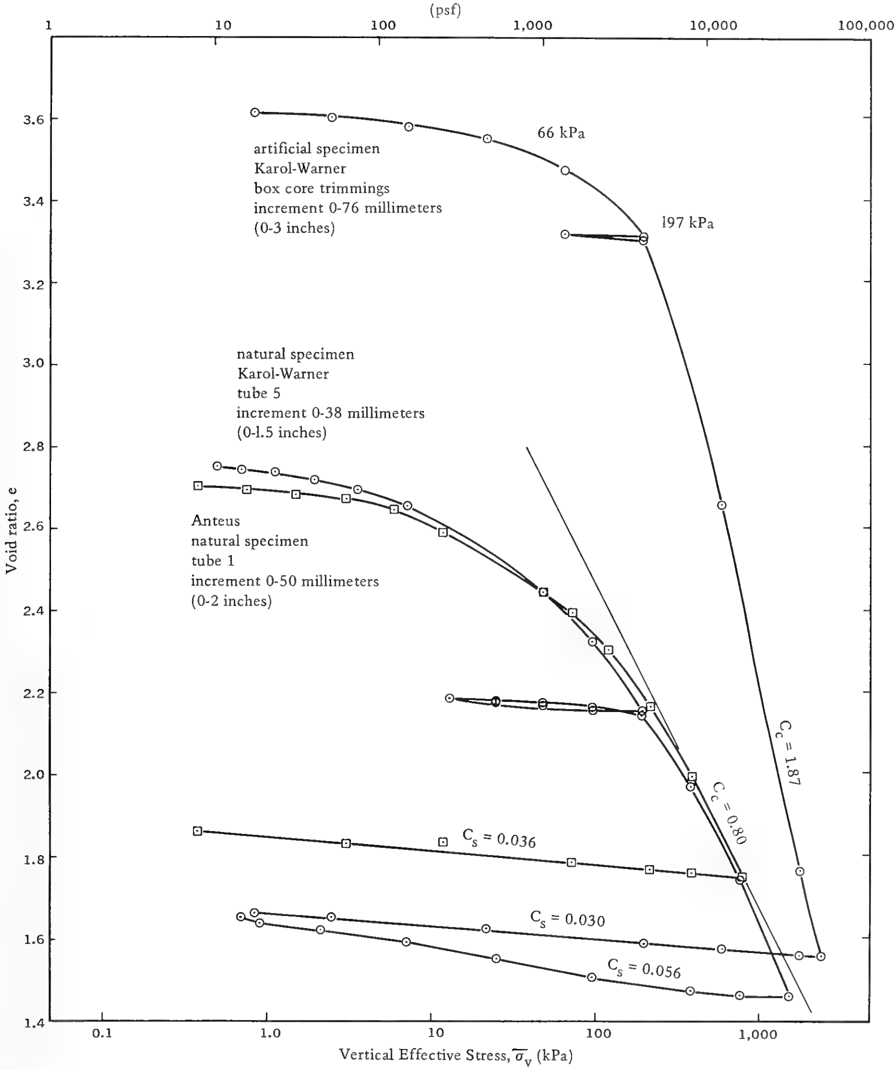

Figure 12. One-dimensional compression test results on three specimens from Box Core 4, indicating grain crushing occurring in artificial sample (no fines).

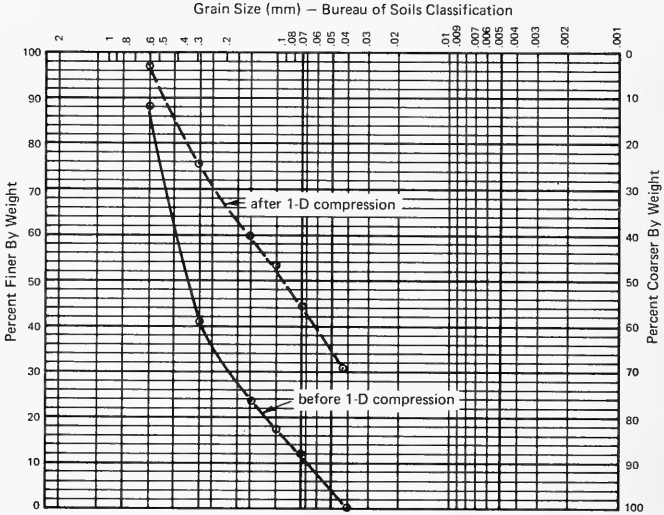

Figure 13. Grain size analysis results on artificial sample used in one-dimensional consolidation test. Sample prepared from trimmings from Box Core 4 retained on No. 325 sieve (0.043 mm).

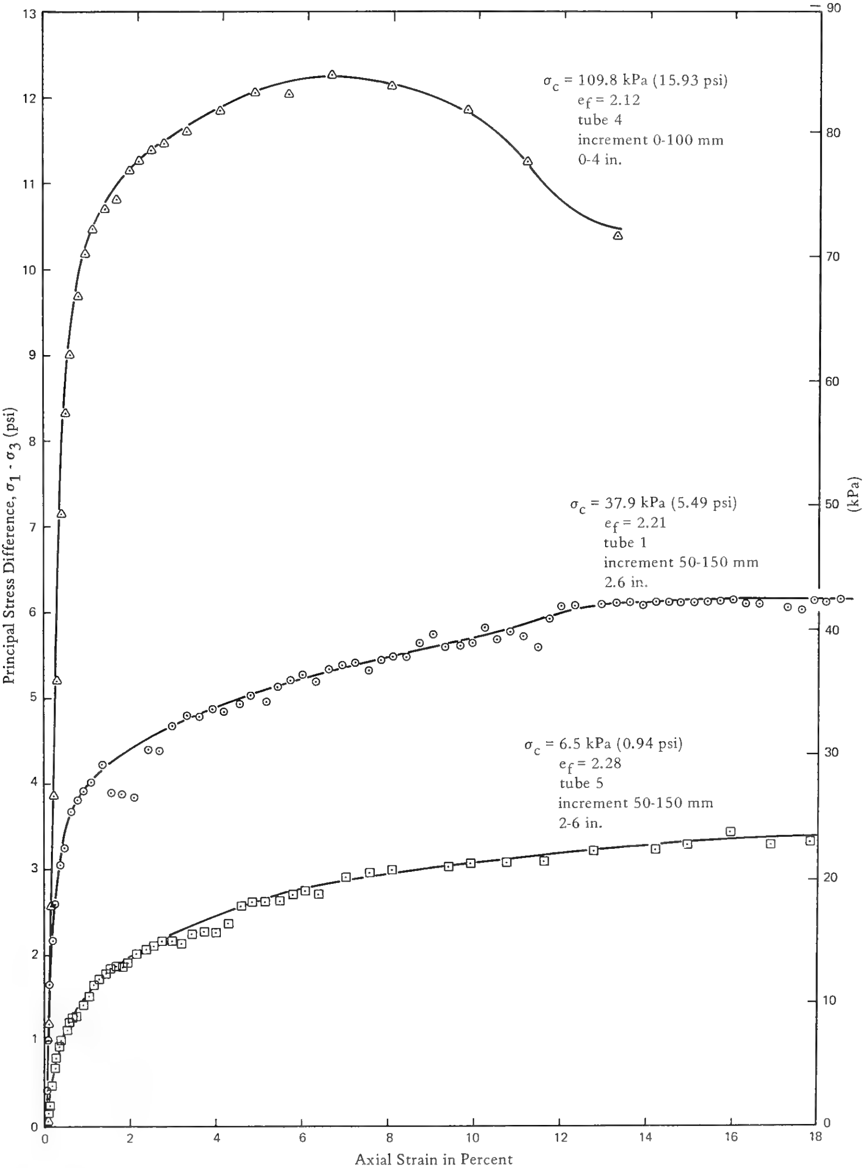

Figure 14. Principal stress difference versus axial strain for specimens consolidated isotropically to different pressures and then sheared undrained by increasing the axial stress, σ_1. Specimens from Box Core 4.

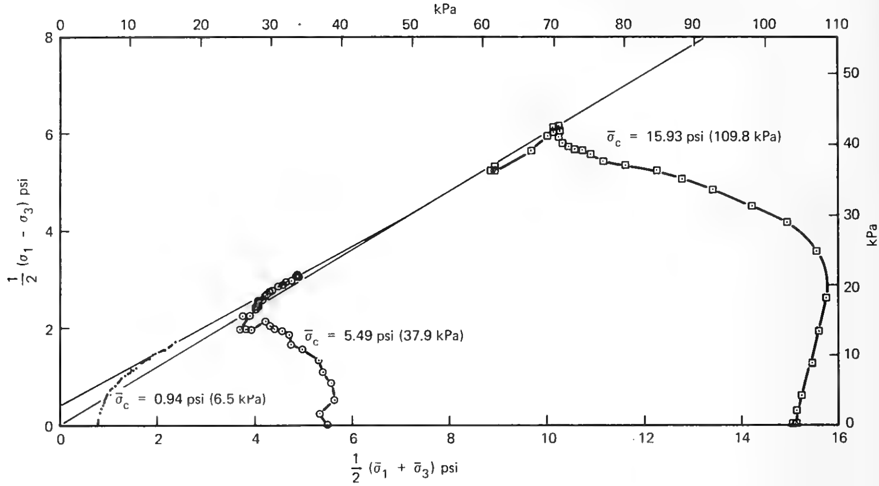

Figure 15. Triaxial specimen ($\overline{CIU}$) stress state during undrained shear for over-consolidated, normally-consolidated, and intermediate behavior.

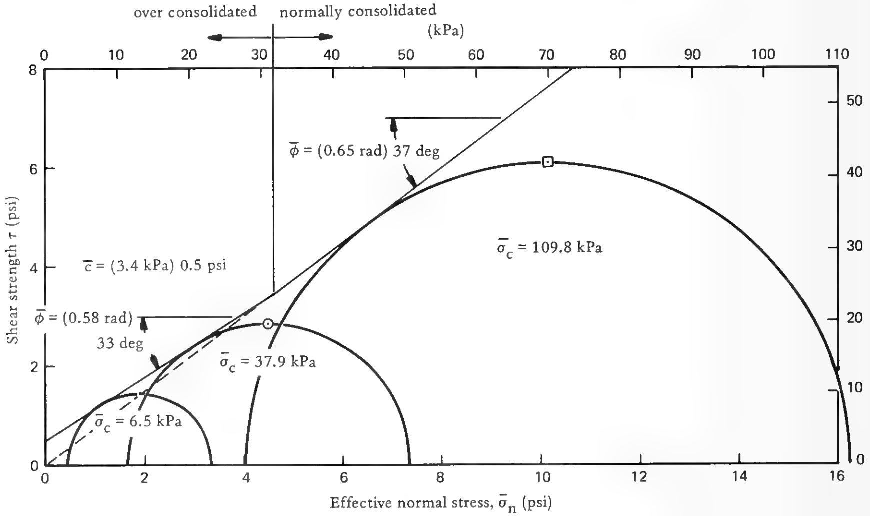

Figure 16. Mohr-Coulomb failure envelope resulting from the triaxial shear strength tests ($\overline{CIU}$) described.

REFERENCES

1. Sverdrup, H.U., Johnson, M.W., and Fleming, R.H., The Oceans, Prentice-Hall, Inc., Englewood Cliffs, New Jersey, 1942, pp. 946-992.

2. Noorany, I. and Gizienski, S.F., ''Engineering Properties of Submarine Soils: State-of-the-Art Review,'' JSMFC, ASCE, Vol. 96, No. SM5, Sept. 1970, pp. 1735-1762.

3. Holmes, A., Principles of Physical Geology, The Ronald Press Co., New York, 1965, pp. 847-855.

4. Lisitzin, A.P., ''Distribution of Carbonate Microfossils in Suspension and in Bottom Sediments,'' in The Micropalaeontology of Oceans, edited by B. M. Funnell and W. R. Riedel, Cambridge University Press, London, 1971, pp. 202-203.

5. Keller, G.H., ''Shear Strength and Other Physical Properties of Sediments from Some Ocean Basins,'' Civil Engineering in the Oceans I, ASCE Conf. Proc., San Francisco, 1967, pp. 391-417.

6. Hironaka, M.C. and Smith, R.J., ''Foundation Study for Materials Test Structure,'' Civil Engineering in the Oceans I, ASCE Conf. Proc., San Francisco, 1967, pp. 489-530.

7. Keller, G.H., ''Mass Properties of the Sea Floor in a Selected Depositional Environment,'' Civil Engineering in the Oceans II, ASCE Conf. Proc., Miami Beach, 1969, pp. 857-877.

8. Einsele, G., ''Sedimentary Processes and Physical Properties of Cores from the Red Sea, Gulf of Aden, and off the Nile Delta,'' Marine Geotechnique, Univ. of Illinois Press, Urbana, 1967, pp. 154-169.

9. Miller, D.G., and Richards, A.F., ''Consolidation and Sedimentation-Compression Studies of a Calcareous Core, Exuma Sound, Bahamas,'' Sedimentology (Amsterdam), Vol. 12, No. 3-4, June 1969, pp. 301-316.

10. Noorany, I., ''Engineering Properties of Submarine Calcareous Soils from the Pacific,'' The International Symposium on the Engineering Properties of Sea-Floor Soils and Their Geophysical Identification, Seattle, July 1971, pp. 130-139.

11. Bryant, W.R., Delaflach, A., and Trabant, P. ''Consolidation of marine clays,'' presented to the ONR Symposium/Workshop on Physical and Engineering Properties of Deep Sea Sediments, Airlie, Virginia, April 1973.

12. Terzaghi, R., ''Compaction of Lime Mud as a Cause of Secondary Structure,'' Journal of Sedimentary Petrology, Vol. 10, No. 2, August 1940, pp. 78-90.

13. Singh, A. and Zen Yang, ''Secondary Compression Characteristics of a Deep Ocean Sediment,'' Proc., International Symposium on the Engineering Properties of Sea-Floor Soils and Their Geophysical Identification, Seattle, 1971, pp. 121-129.

14. Leonards, G.A. and Altschaeffl, A.G., ''Compressibility of Clay,'' JSMFD, ASCE, Vol. 90, No. SM5, Sept. 1964, pp. 133-155.

15. Hansen, J.B., ''A Model Law for Simultaneous Primary and Secondary Consolidation,'' Proc., 5th ICSMFE, Vol. I, Paris, 1961, pp. 133-136.

16. Leonards, G.A. and Girault, P., ''A Study of the One-Dimensional Consolidation Test,'' Proc., 5th ICSMFE, Vol. I, Paris, 1961, pp. 213-218.

17. Poorooshab, H.B., ''Advances in Consolidation Theories for Clays,'' 7th ICSMFE, Vol. III, Mexico, 1969, pp. 491-497.

18. Hansen, J.B. and Inan, S., ''Tests and Formulas Concerning Secondary Consolidation,'' Proc, 7th ICSMFE, Vol. I, Mexico, 1969, pp. 45-53.

19. Leonards, G.A. and Ramiah, B.K., ''Time Effects in the Consolidation of Clays,'' ASTM Spec. Tech. Pub. No. 254, Papers on Soils Meetings, 1959, 1960, pp. 116-130.

20. Buisman, A.S.K., ''Results of Long Duration Settlement Tests,'' Proc., 1st ICSMFE, Vol. I, Cambridge, Mass., USA., 1936, pp. 103-106.

21. Zeevaert, L., ''Consolidation of Mexico City Volcanic Clay,'' ASTM Special Tech. Publ. 232, 1958, pp. 18-32, 381-410.

22. Leonards, G.A., ''Chapter 2: Engineering Properties of Soils,'' Foundation Engineering, ed. by G.A. Leonards, McGraw-Hill, New York, 1962.

23. Singh, A. and Mitchell, J.K., ''General Stress-Strain-Time Function for Soils,'' JSMFD, ASCE, Vol. 94, No. SM1, Jan. 1968, pp. 21-46.

24. Mitchell, J.K., Campanella, R.G., and Singh, A., ''Soil Creep as a Rate Process,'' JSMFD, ASCE, Vol. 94, No. SM1, Jan. 1968, pp. 231-253.

25. Christensen, R.W. and Wu, T.H., ''Analysis of Clay Deformation as a Rate Process,'' JSMFD, ASCE, Vol. 90, SM6, Nov. 1964, pp. 125-157.

26. Noorany, I. and Seed, H.B., ''In-Situ Strength Characteristics of Soft Clays,'' JSMFD, ASCE, Vol. 91, No. SM2, Mar. 1965, pp. 49-80.

27. Walker, L.K., ''Undrained Creep in a Sensitive Clay,'' Geotechnique, Vol. 19, No. 4, Dec. 1969, pp. 515-529.

28. Rosfelder, A.M. and Marshall, N.F., ''Obtaining Large, Undisturbed and Orientated Samples in Deep Water,'' Marine Geotechnique, edited by A.F. Richards, Univ. of Illinois Press, Urbana, 1967, pp. 243-263.

29. Lambe, T.W., Soil Testing for Engineers, John Wiley & Sons, New York, 1951.

30. Noorany, I., ''Measurement of Engineering Properties of Submarine Soils,'' presented to the ONR symposium/workshop on Physical and Engineering Properties of Deep Sea Sediments, Airlie, Virginia, April 1973.

31. Hironaka, M.C., ''Engineering Properties of Marine Sediments near San Miguel Island, California,'' Technical Report R-503, Naval Civil Engineering Laboratory, Port Hueneme, California, December 1966, p. 8.

32. Earth Manual, United States Department of the Interior, Bureau of Reclamation, Denver, Colorado, 1968, pp. 1-18.

33. Taylor, D.W., Fundamentals of Soil Mechanics, John Wiley & Sons, New York, 1948.

34. Altshaeffl, A.G., Associate Professor, School of Civil Engineering, Purdue University, Lafayette, Indiana. Personal communication, June 1973.

35. Peck, R.B., Hanson, W.E., Thornburn, T.H., Foundation Engineering, John Wiley & Sons, New York, 1953, p. 76.

36. Herrmann, H.G., Rocker, K., Jr., and Babineau, P.H., ''Lobster and FMS: Devices for Monitoring Long-Term Seafloor Foundation Behavior,'' Technical Report R-775, Naval Civil Engineering Laboratory, Port Hueneme, California, September 1972, p. 41.

37. Naval Facilities Engineering Command. Design Manual DM-7: Soil Mechanics, Foundations, and Earth Structures. Washington, DC, March 1971.

38. Lambe, T.W. and Whitman, R.V., Soil Mechanics, John Wiley & Sons, New York, 1969.

39. Handbook of Chemistry and Physics, 44th edition, 1962-1963, Chemical Rubber Publishing Co., Cleveland, Ohio, pp. 550-551.

40. Bishop, A.W. and Henkel, D.J., The Measurement of Soil Properties in the Triaxial Test, 2nd edition, Edward Arnold Ltd., London, 1962, p. 96.

41. Seed, H.B., Noorany, I., and Smith, I.M., ''Effects of Sampling and Disturbance on the Strength of Soft Clays,'' Report No. TE-64-1, Institute of Engineering Research, University of California, Berkeley, California, Feb. 1964, p. 22.

42. Skempton, A.W., ''The Pore Pressure Coefficients A and B,'' Geotechnique, Vol. 4, No. 4, 1954, pp. 148-152.

43. The State Institute for Technical Research. Tiedotus. Sarja III - Rakennus. 83 (Report Series III - Building, 83): Investigations on the bearing capacity and engineering properties of silt, by K.V. Helenelund. Helsinki, Finland, 1965, p. 42.

44. Lee, H.J., Senior Project Engineer, Naval Civil Engineering Laboratory, Port Hueneme, California. Personal communication, March 1973.

45. Silva, A., Head, Civil Engineering Department, Worcester Polytechnic Institute, Worcester, Massachusetts. Personal communication, April 1973.

46. Nacci, V.A., Professor, Civil Engineering Department, University of Rhode Island, Kingston, Rhode Island. Personal communication, April 1973.

Appendix

DESCRIPTION OF ONE-DIMENSIONAL CONSOLIDATION TEST AND TRIAXIAL SHEAR TEST

CONSOLIDATION

Consolidation was described earlier as volume change under a state of increased hydrostatic stress, a condition of three-dimensional volume change. Rarely is this condition of consolidation under hydrostatic stress experienced in practice. Instead, the usual consolidation condition is more nearly approximated by one-dimensional vertical volume change. Thus, the usual practice is to run a one-dimensional (1-D) consolidation test on a disc of soil with a diameter-to-height ratio of about three or four [29], as shown in Figure 17. This disc of soil fits snugly into a thick metal ring which limits lateral strain to essentially zero. Loads are applied vertically, in increments, to the soil disc causing the soil pore fluid to be squeezed out and the soil grains to be reoriented into a denser configuration in response to that load. The conventional loading sequence calls for doubling the previous load (Reference 22, p. 149); for instance, if the specimen has been consolidated under a load of 20 newtons, then the next increment of load added would be 20 newtons, raising the total load on the specimen to 40 newtons. Such a loading sequence is termed a ''load-increment ratio'' of 1.

The reduction in soil disc height due to each increment of load is plotted versus the logarithm of time, as shown in Figure 18. Ideally, for a load-increment ratio of 1, this curve has a well-defined inflection point marking the end of primary consolidation and marking that point at which secondary consolidation becomes controlling of the volume change function. The increment of height change for each load increment is used to produce a curve of height change (actually void ratio, e, a function of height change) versus the logarithm of vertical effective stress, called an e-log $\bar{\sigma}_v$ curve, as shown in Figure 12. In practice, these data plots are then interpreted to predict the total settlement of the soil surface at any point in time due to an applied vertical load.

TRIAXIAL SHEAR

A commonly used and widely accepted test configuration for soil shearing deformations and soil failure strength is the triaxial shear test [40] in which a cylindrical specimen of soil, of length-to-diameter ratio 2 or 2-1/2:1 (Reference 22, p. 192) is subjected to a hydrostatic stress state by a confining fluid and to a superimposed axial stress by a loading ram (see Figure 19). The soil specimen is capped at its ends by porous discs which permit passage of water out of the sample to a closed volume change and pressure measuring system. The specimen and discs are sealed off from the surrounding confining fluid by a rubber sleeve. The confining stress, σ_3, applied via the surrounding cell fluid, is resisted within the soil specimen by two components: partly by the specimen pore fluid, as a specimen pore pressure, u (see Figure 19); and partly by the specimen soil structure, as an effective minor principal stress, $\bar{\sigma}_3$. An additional axial stress, σ_d, is superimposed on this isotropic system by the axially-acting loading ram, such that the axial total stress applied to the specimen is $\sigma_1 = \sigma_d + \sigma_3$ and the axial effective stress is $\bar{\sigma}_1 = \sigma_d + \bar{\sigma}_3$. If the axial stress is greater than the confining stress, then $\bar{\sigma}_1$ is, more properly, the effective major principal stress (Reference 38, pp. 117-119).

Soil specimens of this series were first subjected to a hydrostatic confining stress, σ_3, and the specimen pore water was allowed to drain into a volume change measuring device, at least until the end of primary consolidation had been attained, as dictated by a triaxial volume change versus time plot (similar to Figure 18), i.e., the end of primary consolidation was noted by a slope change in the volume change data plot. Then the specimen was sealed off from the drainage system, the confining pressure, σ_3 was maintained, and the specimen was loaded axially, until shear failure occurred (Reference 29, pp. 125-126). Shear failure was defined herein as occurring at the maximum principal stress difference, $(\sigma_1-\sigma_3)_{max} = \sigma_d$ max (Reference 22, p. 177). This type of test is referred to herein as a $\overline{\text{CIU}}$ test, that is, consolidated isotropically and sheared undrained.

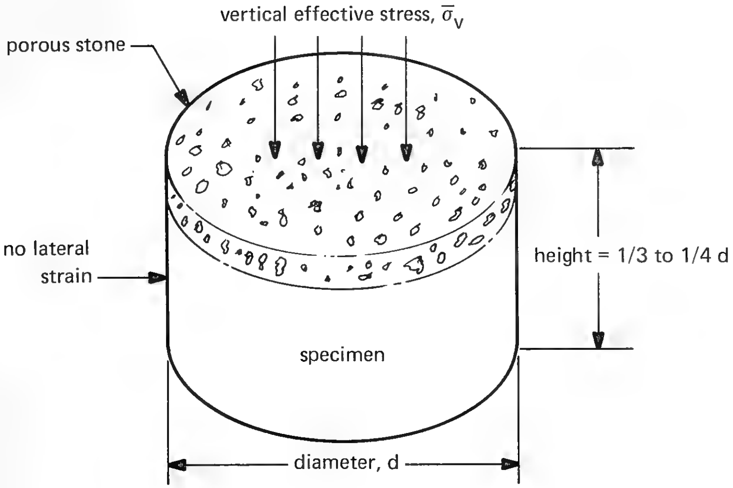

Figure 17. Idealization of consolidation test specimen.

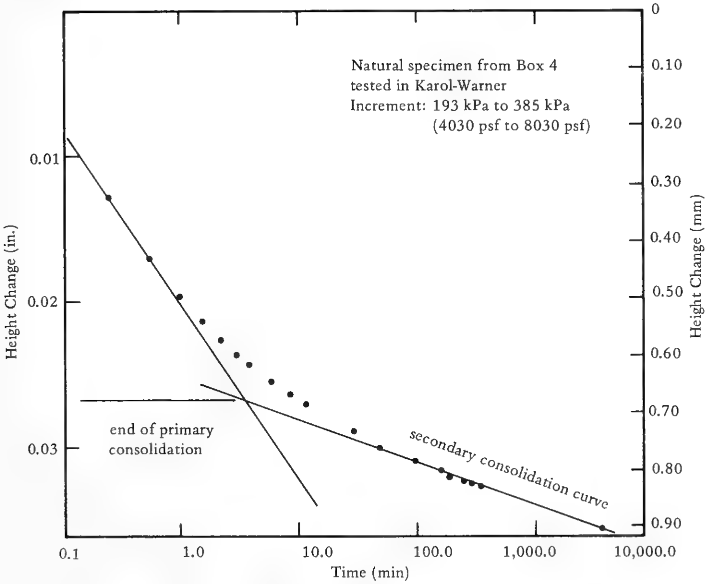

Figure 18. Typical curve of height change versus logarithm of time for an increment of load applied to one-dimensional consolidation specimen. Such a curve is used in identifying the end of primary consolidation. (The curve is called a Terzaghi Type I curve [16].)

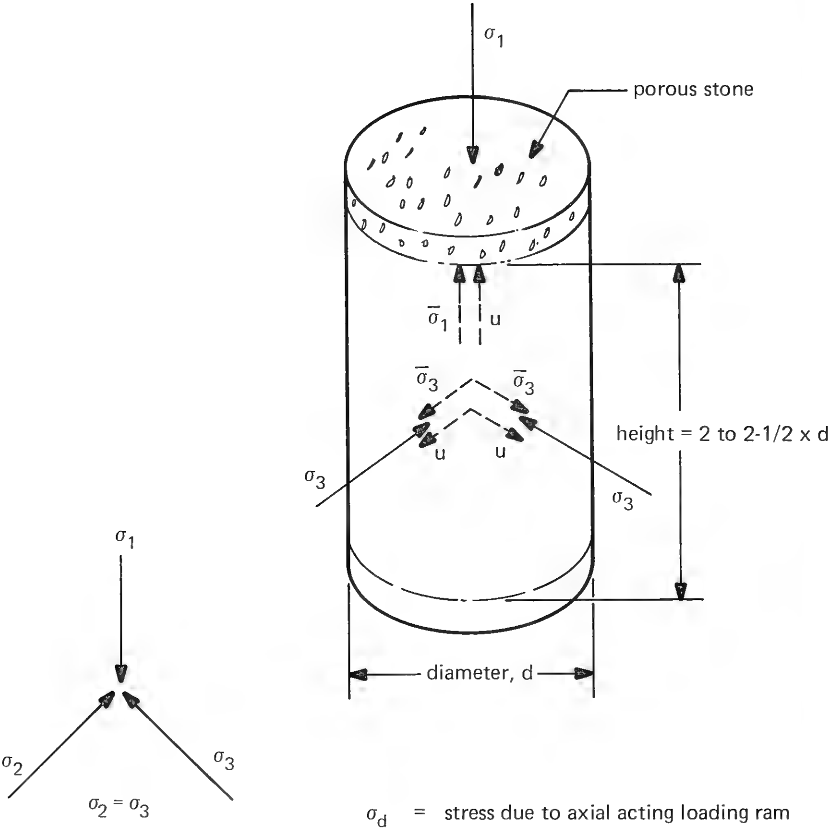

σ_d = stress due to axial acting loading ram

$\sigma_1 = \sigma_3 + \sigma_d$

$\bar{\sigma}_1 = \bar{\sigma}_3 + \sigma_d$

Figure 19. Idealization of triaxial test specimen.

List of Symbols

A_f	Skempton's A-parameter at failure
C_c	Compression index
C_s	Swelling index
C_α	Coefficient of secondary consolidation
$\overline{CIU}$	Consolidated isotropically and sheared undrained with pore pressure measurements
$\bar{c}$	Effective cohesion
c_v	Coefficient of consolidation
d	Diameter of specimen
e	Void ratio
e_f	Void ratio at end of test
e_o	Initial void ratio
H	Specimen height at end of primary consolidation
ΔH	Specimen height change during secondary consolidation
t	Time increment
u	Pore pressure
w	Initial water content
w_L	Liquid limit
w_P	Plastic limit
σ_d	Axial stress due to load ram in triaxial test
σ_1	Total axial stress on triaxial specimen, total major principal stress
σ_3	Total lateral stress on triaxial specimen, total minor principal stress
$\bar{\sigma}_c$	Isotropic consolidation stress
$\bar{\sigma}_v$	Vertical effective stress
$\bar{\sigma}_1$	Effective axial stress on triaxial specimen, effective major principal stress
$\bar{\sigma}_3$	Effective lateral stress on triaxial specimen, effective minor principal stress
$\bar{\phi}$	Effective angle of internal friction
1-D	One-dimensional

DISTRIBUTION LIST

SNDL Code	No. of Activities	Total Copies	
--	1	12	Defense Documentation Center
--	1	10	Office of Naval Research
FKAIC	1	2	Naval Facilities Engineering Command
FKN1	6	6	NAVFAC Engineering Field Divisions
FKN5	9	9	Public Works Centers
FA25	1	1	Public Works Center
--	9	9	RDT&E Liaison Officers at NAVFAC Engineering Field Divisions and Construction Battalion Centers
--	253	253	CEL Special Distribution List for persons and activities interested in reports on Ocean Engineering